Impact of Channel Sounder Frequency Offsets On The Estimation of Channel Parameters

Min Lin and Ian Wassell
University of Cambridge, Computer Laboratory,
Cambridge, UK
ml406@cam.ac.uk ijw24@cam.ac.uk

Abstract-We investigate the design of a multiple input multiple output (MIMO) channel sounder appropriate for the broadband fixed wireless access (FWA) scenario. To this end a 4 transmit 4 receive antenna system was simulated in order to investigate the effect of equipment imperfections on the estimation of channel parameters, for example, *K*-factor, power delay profile (PDP), antenna correlation coefficients (ACC) and signal angle of arrival (AOA). The channel employed in the simulation is based on the SUI-3 model [8]. The accuracy of the channel estimation results is dependent upon the frequency offset between the phase lock loop (PLL) reference oscillators used at the transmitter and receiver. Consequently, high cost rubidium reference sources are usually used since they can reduce the frequency offset to almost zero owing to their frequency stability (aging) of about 5×10^{-10} per year [13], equivalently, 5×10^{-4} *ppm* per year. We wish to determine how much frequency offset can be tolerated before the estimation results become unacceptable. To this end we have conducted extensive system simulations that have revealed that acceptable accuracy can be achieved using relatively low performance and therefore inexpensive reference sources.

Keyword**:** MIMO channel modeling, Channel Sounder, Antenna Correlation Coefficients, Power Delay Profile, Angle of Arrival, Crystal reference, Frequency offset, Phase Lock Loop.

I. INTRODUCTION

Channel models are essential for the analysis and simulation of wireless systems. To have efficient baseband designs for communication systems, we need to have accurate channel characteristics. A channel sounder should provide accurate and high resolution measurement data for the purpose of developing realistic simulation models. However, in order to reduce cost and complexity, most commercial multiple input multiple output (MIMO) channel sounders use a single, time-division multiplexing (TDM) switching scheme [1]. As a result, frequency offset as well as phase noise effects will introduce some inaccuracy into the measurement results. The purpose of the investigation conducted here is to quantify the effects due to frequency offset.

The MIMO channel sounder to be developed is intended for vector channel sounding in outdoor fixed wireless access (FWA) environments in the 3.5 GHz band using a 4 transmit-4 receive i.e., a 4×4 multiple antenna configuration. The transmitter and receiver are frequency and time synchronized using a training sequence (TSEQ) sent from the transmitter.

Following TSEQ, particular known data sequences are transmitted in order that the channels between individual antenna pairs may be measured. After capturing the complex baseband raw data in real time, the data is stored for off-line post-processing. The post-processing software takes the stored data to estimate the required channel parameters, for example multi-path delay spread, power delay profile (PDP), angle of arrival (AOA), *K*-factors, and the antenna cross-correlation coefficients (ACCs).

There are a number of publications concerning FWA channel modeling, but those which address channel sounder impairments are still quite rare. However, the effects of phase noise on the accuracy of MIMO channel capacity measurements was investigated in [2], and the impact of imperfect system response on rms delay spread measurements at 2.6 GHz using a 2×8 MIMO wireless channel sounder was analyzed in [3].

In this paper, we present simulation results concerning the effects of frequency offset on the estimation of channel parameters using a test channel based on the SUI-3 model. The results of this investigation will serve as a reference during the development of the actual channel sounder. In section II, we briefly describe the arrangement of the channel sounder, the wideband channel models employed in the simulations and the estimation techniques used in the off-line post-processing. In section III we introduce frequency offset into the simulation model. The accuracy of the estimation results as a function of the frequency stability of the reference clocks will be presented and discussed in section IV. The paper is concluded in section V.

II. SIMULATION MODEL

A. MIMO Channel Sounder Structure

The structure of our TDM MIMO channel sounder is depicted in Fig.1.

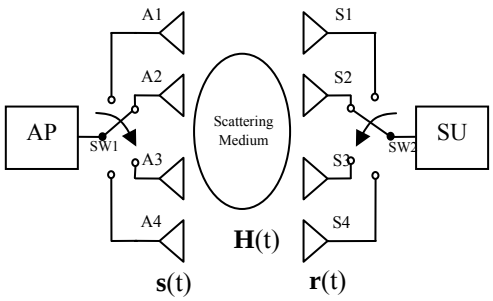

Fig.1 Structure of a TDM MIMO Channel Sounder

The access point (AP) and subscriber unit (SU) are each connected to an array of four antennas through switches SW1 and SW2 respectively. The AP periodically transmits a training sequence (TSEQ) followed by a number of Multi-Element Sounding (MES) sequences. For the 4×4 sounder, four MES sequences are sent, yielding the structure shown in Fig.2.

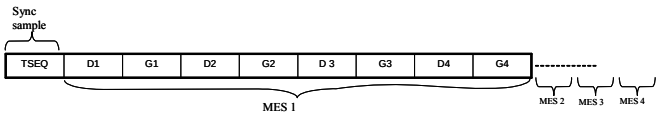

Fig.2 MES sequence structure for the transmission scheme

The MES sequence consists of four data sounding sequences each separated by guard intervals. The data sounding sequence elements (D1 to D4) are each transmitted by the specified antenna. These sequences are unique and have been selected to have good auto- and cross- correlation properties [11]. The guard intervals (G1 to G4) are used to mitigate the effects of multi-path propagation and also to provide time for the AP to switch antennas prior to transmission of the next data sequence. Each data sequence has 128 symbols and the guard interval is 150 symbols long. Note that the transmission symbol rate is 10Mbps and the receiver sampling frequency is 40MHz giving 512 samples for the TSEQ and data sequences and 600 samples for the guard intervals at the receiver. The SU receives one MES sequence before switching to the next receive antenna. The TSEQ is used by the SU to obtain frequency and timing synchronisation. It is the effect on estimation performance of the frequency offset remaining after synchronisation which is our concern here.

B. Wideband Channel Model

In this section, we describe the wideband channel simulation model. The signals at the AP transmit antenna array are denoted

$$\mathbf{s}(t)=\left[s_1(t),s_2(t),...,s_{M_T}(t)\right]^T, \tag{1}$$

where $s_m(t)$ is the signal at the m^{th} antenna connector. Likewise, the signals at the SU receiver antenna array are the components of the vector

$$\mathbf{r}(t)=\left[r_1(t),r_2(t),...,r_{N_R}(t)\right]^T. \tag{2}$$

The wideband MIMO radio channel can be expressed as

$$\mathbf{H}(t)=\sum_{l=1}^{L}\mathbf{G}_l\delta(t-\tau_l) \tag{3}$$

where $\mathbf{H}(t)\in\mathbb{C}^{M_T\times N_R}$, L is the number of tap delays, and

$$\mathbf{G}_l=\begin{bmatrix} g_{11}^l & g_{12}^l & \cdots & g_{1N_R}^l \\ g_{21}^l & g_{22}^l & \cdots & g_{2N_R}^l \\ \cdots & \cdots & \cdots & \cdots \\ g_{M_T1}^l & g_{M_T2}^l & \cdots & g_{M_TN_R}^l \end{bmatrix}_{M_T\times N_R} \tag{4}$$

is a complex matrix which describes the linear transformation between the transmit and receive antenna array at delay τ_l, where g_{mn}^l is the complex transmission coefficient from the m^{th} AP transmit antenna to the n^{th} SU receive antenna. It can be seen that a tapped delay line model has been used to represent the L resolvable delay paths in each channel. We also assume that the average power of the transmission coefficients is identical for a given delay, so

$$P_l=E\left\{\left|g_{mn}^l\right|^2\right\} \tag{5}$$

for all $n\in\left[1,2,...,N_R\right]$ and $m\in\left[1,2,...,M_T\right]$ and the coefficients are uncorrelated from one delay to another, so

$$\left\langle\left|g_{mn}^{l_1}\right|^2,\left|g_{mn}^{l_2}\right|^2\right\rangle=0 \quad \text{for } l_1\neq l_2 \tag{6}$$

where $\langle a,b\rangle$ denotes the correlation coefficient between a and b. These assumptions satisfy the requirement described in [7], i.e., the fading in the individual channel should have low cross-correlation and the mean power available from each channel should be almost equal. The channel parameters used are those demanded by the SUI-3 model [8].

We use this channel simulation model when we evaluate the performance of the channel impulse response (CIR) and Power Delay Profile (PDP) estimation algorithms which are implemented in the off-line post-processing software described in [9]. We also modified the off-line post-processing software for use with the MIMO system, and further developed it to estimate the correlation coefficients between antennas and also the angle of arrival (AOA). This will be described in the next section.

C. Simulation of Antenna Correlated Channel

In this section, we introduce the technique by which we include the effect of antenna correlation in the channel model. We then introduce our approach for estimating AOA.

There are a number of assumptions that we have to take into consideration when introducing antenna correlation into the channel model. Since we are using the SUI-3 model, there are three taps corresponding with the three resolvable paths. Firstly, we assume that equivalent taps in all channels have equal power:

$$\sigma_{xl}^2=\sigma_{yl}^2=\sigma_l^2, l\in\left[1,2,3\right] \tag{7}$$

where, l denotes the tap number and x and y denote the AP and SU antenna indices respectively.We also assume that paths (i.e., taps) with different delays are uncorrelated within a channel as well as between channels,

i.e.: $\rho_{xy}=E\left\{h_{xk}(t)h_{yl}^*\right\}=0,\ \forall k\neq l$ where $k,l\in\left[1,2,3\right]$. (8)

Lastly, we assume that the matrix containing the antenna correlation coefficients is symmetrical. i.e.,: $\rho_{xy} = \rho_{yx}$.

We can then represent all correlation coefficients for all antenna pairs at both transmitter and receiver using two correlation matrices, namely $\mathbf{R}_{tx}$ and $\mathbf{R}_{rx}$ respectively where,

$$\mathbf{R}_{tx} = \begin{bmatrix} 1 & \rho_{12}^{tx} & \rho_{13}^{tx} & \rho_{14}^{tx} \\ \rho_{21}^{tx} & 1 & \rho_{23}^{tx} & \rho_{24}^{tx} \\ \rho_{31}^{tx} & \rho_{32}^{tx} & 1 & \rho_{34}^{tx} \\ \rho_{41}^{tx} & \rho_{42}^{tx} & \rho_{43}^{tx} & 1 \end{bmatrix} \text{ and } \mathbf{R}_{rx} = \begin{bmatrix} 1 & \rho_{12}^{rx} & \rho_{13}^{rx} & \rho_{14}^{rx} \\ \rho_{21}^{rx} & 1 & \rho_{23}^{rx} & \rho_{24}^{rx} \\ \rho_{31}^{rx} & \rho_{32}^{rx} & 1 & \rho_{34}^{rx} \\ \rho_{41}^{rx} & \rho_{42}^{rx} & \rho_{43}^{rx} & 1 \end{bmatrix}.$$

We also propose an enhanced model which introduces angular information into the ACCs using equation (9) for the Rayleigh channel [4], and equation (10) for the Rician channel [5]. The Rayleigh model that we used was based on [15]. Consequently, the correlation coefficient between each pair of antennas depends upon AOA, antenna spacing and angular spread. So,

$$\rho_{Rayleigh} \approx e^{-j2\pi(p-q)\frac{d}{\lambda}\sin(\theta)} \times e^{-\frac{1}{2}\left(2\pi(p-q)\frac{d}{\lambda}\cos(\varphi)\right)^2} \quad (9)$$

$$\rho_{Rician} \approx e^{-j2\pi(p-q)\frac{d}{\lambda}\sin(\theta)}, \quad (10)$$

where, θ is mean angle of arrival and φ is the angular spread of the associated scattering cluster.

Note that equation (9) is valid provided φ is small [4]. As we have applied the Gaussian Angle of Arrival (GAA) model, which is a special case for Gaussian Wide Sense Stationary Uncorrelated Scattering (GWSSUS) model [16], the AOA is assumed to be Gaussian distributed with a certain angular spread, φ.

For the SUI-3 model, the ratio between the dominant power and the scattering power, known as *K*- factor is 1 for the LOS path (i.e., the first path) and 0 for the remaining non-LOS (NLOS) paths. Therefore, we need to modify (9) and (10) such that they take the *K*-factor into consideration. For the LOS path, the dominant power, P_d and scattering power, P_s are equally split since $K = 1$. Therefore, the correlation coefficient for the LOS path is

$$\rho_{LOS} = \frac{K}{K+1}\rho_{Rician} + \frac{1}{K+1}\rho_{Rayleigh} \quad (11)$$

$$\rho_{LOS} = \frac{1}{2}\rho_{Rician} + \frac{1}{2}\rho_{Rayleigh}.$$

Note that $\rho_{NLOS1} = \rho_{NLOS2} = \rho_{Rayleigh}$. This is so because $K = 0$ for the two NLOS components. A detailed derivation of these two types of correlation coefficients can be found in [11]. With the previous definition of the correlation matrices for both transmit and receive antennas, we can then simulate correlated channels using the model proposed in [8], i.e.,

$$\mathbf{H} = \mathbf{R}_{rx}^{1/2}\mathbf{H}_c\mathbf{R}_{tx}^{1/2}. \quad (12)$$

However, it should be noted that there is a more sophisticated way of implementing the correlated channel, using the Kronecker product as described in [12]. From (9) and (10), it is clear that angular information is embedded within the antenna correlation coefficient matrix, therefore to estimate the AOA, we first have to estimate the ACC. To estimate the ACC, we use the approach proposed in [10], i.e., for two particular antennas, *x* and *y*

$$\rho_{xy} = \left| \frac{\rho_1\sigma_1^2 + \rho_2\sigma_2^2 + \rho_3\sigma_3^2}{\sigma_1^2 + \sigma_2^2 + \sigma_3^2} \right|, \quad (13)$$

where, ρ_l are the correlation coefficients between each of the 3 pairs of taps $h_{xl}(t)$ and $h_{yl}(t)$, and σ_l^2 denotes the power of each of the taps, $l \in [1,2,3]$:

$$\rho_l = \frac{E\left\{h_{xl}(t)h_{yl}^*(t)\right\}}{\sqrt{\sigma_{xl}^2\sigma_{yl}^2}}, l \in [1,2,3], \quad (14)$$

Based upon the assumption in (7), i.e., $\sigma_{xl}^2 = \sigma_{yl}^2 = \sigma_l^2$.

The estimation results obtained using (13) and (14) in our off-line post-processing software can be validated by comparing the estimated ACCs with the ones yielded by (9) and (10). Once we have estimated the correlation matrices, the AOA can be estimated using TLS ESPRIT algorithm [6] [17] [18]. Unfortunately, space limitations preclude a detailed description of this technique. In the next section, we will describe the effect of frequency offset, and show via simulation how it influences the estimation accuracy of the CIRs, ACCs and AOAs.

III. EFFECT OF FREQUENCY OFFSET

In general, published work concerning channel measurement and characterization, assumes that the frequency offset between the transmitter and receiver is zero, since it is usual to employ rubidium reference clocks. However, rubidium clocks are very expensive and so it is worthwhile considering if other less expensive oscillators may be used. The frequency offset (i.e., phase rotation observed at the receiver) is caused by differences in the oscillator reference frequencies at the transmitter and receiver. The frequency shift depends upon the frequency stability of the reference clocks usually specified in terms of part per million (*ppm*). If both transmitter and receiver have different clock accuracies, then the maximum frequency inaccuracy in terms of *ppm* is

$$f_{ppm(\max)} = f_{ppm(\max)rx} + f_{ppm(\max)tx}. \quad (15)$$

So the maximum phase rotation over a received bust having *N* samples with a sample rate, r_s owing to the frequency offset, is given by:

$$\theta_{\max} = \left(2\pi \times f_c \times f_{ppm(\max)}\right) \times \frac{N}{r_s}, \quad (16)$$

where, f_c denotes the nominal carrier frequency. Consequently, the incremental phase rotation for each received sample is:

$$\theta_i = \frac{\theta_{\max}}{N}. \quad (17)$$

For our case, the frequency stability, f_{ppm} following the frequency synchronization process at the SU is equivalent to 0.1 *ppm*. This is because during the training process the SU's PLL is driven to match the frequency of the AP's and when they are locked, the maximum frequency offset, f_{Δ} is around 300Hz. Consequently the frequency stability is

$$f_{ppm} = \frac{f_{\Delta}}{f_c} = \frac{300Hz}{3.5GHz} = 0.1\times10^{-6}\,(\text{i.e., } 0.1ppm). \qquad (18)$$

Referring to the sequence structure in Fig.2, we have total of 4448 samples for each MES sequence. As we are switching between four SU antennas, we send a total of 4 MES sequences yielding $4448\times4 = 17792$ data and guard samples at the receiver. Including TSEQ (512 samples) at the beginning for synchronization, we have a total of 18304 samples at the receiver at a sample rate of 40Mbps. Consequently, the maximum phase rotation, $\theta_{\max} = 1.0063rad$ after TSEQ and all the MESs are received. The simulation results will be presented in the next section.

IV. SIMULATION RESULTS

In this section, we present the effects of frequency offset on the estimation of PDPs, ACCs and AOAs. Antenna spacings of $\Delta = 0.5\lambda$ have been used.

A. Impact on Power Delay Profile (PDP) Estimation Results

In *Fig.6*, we present the estimated PDPs for four frequency stability values, (i.e.,f_{ppm} = 0, 0.04, 0.08, 0.1). Due to limited space and since other channels are similar, we only present the results for one channel. The theoretical RMS delay spread is 0.26373μsec while the estimated RMS delay spread is around 0.296 μsec for all the presented values of frequency offset. From these results, we can see that the frequency stability has almost no effect on the PDPs. The three paths can still be resolved since the residual convolution components are all below 5 dB. This is important, because if we cannot resolve the significant paths then it will be very difficult to estimate other parameters such as ACCs and AOAs.

B. Impact of frequency offset on ACC Estimation

In this section, mean square error (MSE) results are presented for 30 complete realizations (i.e., 30 transmissions each having 1 TSEQ and 16 MES sequences). *Fig.3* and *Fig.4* present the mean squared error (MSE) of the estimated magnitude and phase for the ACCs of the LOS component. It can be seen that worsening frequency stability has an insignificant effect on the magnitude of the ACCs. From *Fig.4*, it is clear that the MSE of the ACC phase grows larger with worsening frequency stability. The results presented in *Fig.3* and *Fig.4* show that the impact of frequency offset on the estimation of ACCs is relatively insignificant. Next, we are interested to see if this has an effect on the AOA estimation.

C. Impact of frequency offset on Angle of Arrival (AOA) Estimation

We present the results at a constant antenna spacing of 0.5λ since this ensures no ambiguity in the AOA estimation results [14]. The AOAs are measured in degree. From the simulation results presented in *Fig.5*, the MSE at f_{ppm} = 0.1*ppm* is approximately 2.79. It can be observed that the MSE of the AOA increases as frequency stability worsens. This is to be expected since the estimation of AOA is heavily dependent on the phase of the received signal. *Fig.5* provides a means for us to choose an appropriate crystal clock depending upon the accuracy required by the application. That is we can trade-off performance against cost.

V. CONCLUSION

In this paper, we introduced the structure of our channel sounder, simulation model, and our approach for estimating the channel parameters such as PDPs, ACCs and AOAs. We then presented our results concerning the impact of frequency offset. We can see that the impact of the frequency offset on the accuracy of the estimation results is not large even when f_{ppm} = 0.1*ppm*. As a result, we conclude that the use of rubidium clocks is not necessary in our application. Consequently, the simulation results show that it is possible to construct a low cost MIMO channel sounder using inexpensive reference sources. In our investigation, we have not yet considered some factors which we will include in future simulations. First, we have only considered the impact in a high SNR regime and only consider the effect on the LOS component, where the angular spread is quite small. The angular spread for the NLOS components is relatively large and may impact the accuracy of AOA estimation. We are currently investigating how large is the angular spread that can be tolerated with a frequency stability of 0.1*ppm*. For another, the phase noise owing to the VCO will also be considered. A possible approach to reduce the effect of the phase noise is to use a Wiener filter, as proposed in [19]. Having validated our sounder and off-line processing techniques, we will then under take a programme of practical measurements.

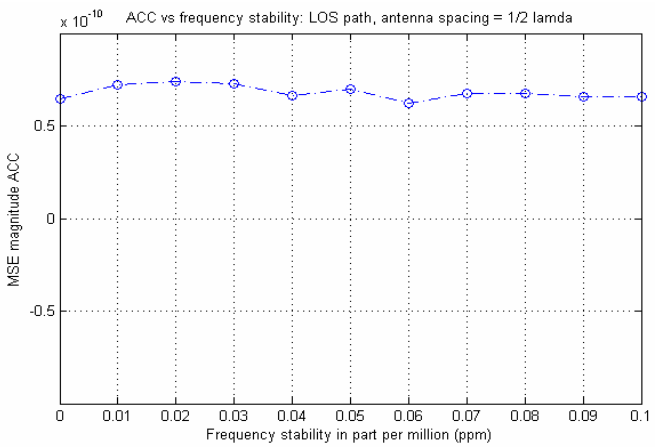

Fig.3 Impact on magnitude of ACC

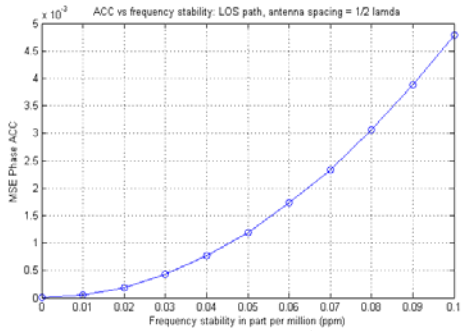

Fig.4 Impact on phase of ACC

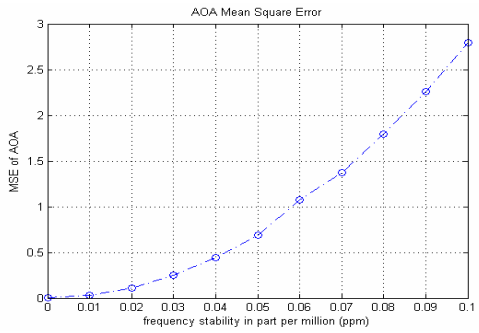

Fig.5 Mean Square Error of AOA with worsening frequency stability

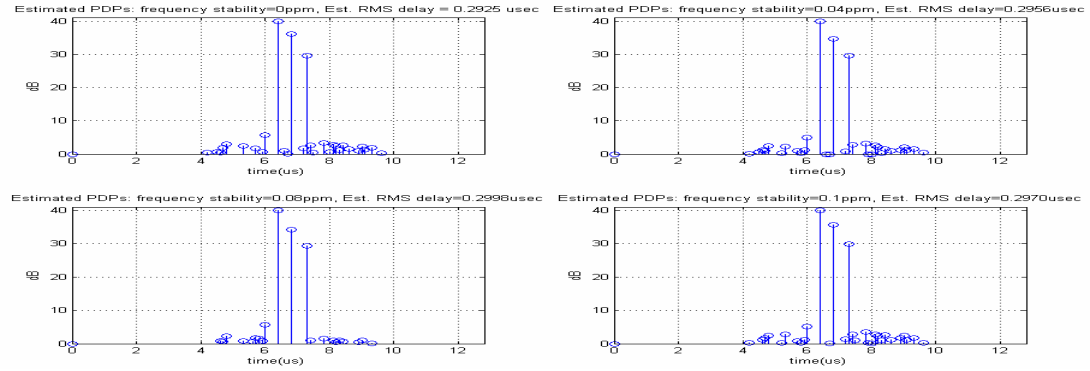

Fig.6 Impact on PDPs with varying frequency stability

REFERENCE

[1] MEDAV RUSK MIMO Channel Sounder, http://www.channelsounder.de/

[2] Daniel S. Baum and Helmut Bolcskei, "Impact of Phase Noise on MIMO Channel Measurement Accuracy", *Communication Technology Laboratory, Swiss Federal Institute of Techonology* , Swizerland, IEEE 2004.

[3] Hyun Kyu Chung, Niko Vloeberghs, Heon Kook Kwon, Sung Jun Lee, Kwang Chun Lee, Mobile Telecommunication Research Laboratory, ETRI, "MIMO Channel Sounder Implementation and Effects of Sounder Impairment on Statistics of Multipath Delay Spread". *IEEE VTC* 2005

[4] David Asztely, "On Antenna Arrays in Mobile Communication Systems Fast Fading and GSM Base Station Receiver Algorithms", IR-S3-Sb_9611, Royal Institute of Technology, Department of Signals, *Sensors & Systems Signal Processing*, March 1996.

[5] A. Abdi and M. Kaveh, "A Space-Time Correlation Model for Multielement Antenna Systems in Mobile Fading Channels", *IEEE Journal on Selected Areas in Communications*, Vol. 20, No.3, April 2002, pp.550-560.

[6] Richard Roy and Thomas Kailaith, Fellow, "ESPRIT – Estimation of Signal Parameters Via Rotational Invariance Techniques", *IEEE TRANSACTIOSN ON ACOUSTICS, SPEECH, AND SIGNAL PROCESSING*. VOL. 37, NO. 7 JULY 1989.

[7] Simon R. Saunders "Antenna and Propagation for Wireless Communication Systems", *WILEY*, 1999.

[8] V.Erceg et.al, "Channel Model for Fixed Wireless Applications*I*", *IEEE 802.16 Broadband Wireless Access Working Group*, 27 June 2003.

[9] C. L. Hong, I. J. Wassell, G. E. Athanasiadou, S. Greaves, M. Sellars, "Wideband channel measurements and characterisation for broadband wireless access". *Twelfth International Conference on Antennas and Propagation*, 2003 (ICAP 2003), Volume 1, Pages 429-432, IEE Press, April 2003.

[10] Jean Philippe Kermoal, Laurent Schumacher, et al, "A Stochastic MIMO Radio Channel Model with Experimental Validation", *IEEE Journal on selected areas in communications*. Vol. 20, No. 6, August 2002.

[11] E. K. Bartsch, "Equalization and Space-Time Processing For Fixed Broadband Wireless Access Systems", *PhD Thesis*, *University of Cambridge*.

[12] Jean Philippe Kermoal, Laurent Schumacher, Member, IEEE, Kalus Ingemann Pedersen, Member, IEEE, Preben Elgaard Mogensen, Member, IEEE, and Frank Frederiksen, "A Stochastic MIMO Radio Channel Model With Experimental Validation". *IEEE JOURNAL ON SELECTED AREAS IN COMMUNICATIONS*, VOL. 20, NO.6, AUGUST 2002.

[13] AccuBeat Ltd. Accurate Frequency and Time, *Specifications – AR-100B Data sheet*, 26 June 2003.

[14] Bjorn Ottersten, Member, IEEE, Mats Viberg, Member, IEEE and Thomas Kailath, Fellow, IEEE, "Performance Analysis of the Total Least Squares ESPRIT Algorithm", *IEEE TRANSACTIONS ON SIGNAL PROCESSING*, VOL. 39, NO.5, MAY 1991.

[15] F. Adachi et al, "Cross correlation between the envelopes of 900 MHz signals received at a mobile radio base station site". *IEE Proceeding*, 133(6): 506-512, October 1986.

[16] Richard B. Ertel and Paulo Cardieri, Virginia Polytechnic Institute, Kevin W. Sowerby, University of Auckland, New Zealand, Theordore S. Rappaport and Jeffrey H. Reed, Virginia Polytechnic Institute, "Onverview of Spatial Channel Models for Antenna Array Communication Systems", *IEEE Personal Communications*, Februray 1998.

[17] Charles W. Therrien, "Discrete Random Signals and Statistical Signal Processing", *Prentice-Hall International Edintions*, 1992.

[18] Todd K. Moon Wynn C. Stirling, "Mathematical Methods and Algorithms for Signal Processing", *Prentice-Hall*, 2000.

[19] Niels Hadaschik, Meik Dorpinghaus, Andrea Senst, Ole Harmjanz, Uwe Kaufer, Gerd Ascheid, Heinrich Meyr, "Improving MIMO Phase Noise Estimation By Exploiting Spatial Correlations", *IEEE International Conference on Acoustics, Speech and Signal Processing (ICASSP 2005)*, Philadelphia, PA, USA, March 2005